

## 基于改进灰度重心法的轨道扣件重构与故障诊断

肖圳, 孙世政\*, 郑天成, 庞珂, 魏子杰

重庆交通大学机电与车辆工程学院 重庆 400074

**摘要** 针对轨道扣件表面结构复杂导致的线结构光照射分布不均匀问题,研究了一种基于改进灰度重心法的光条中心线提取方法,精准重构了轨道扣件点云模型。基于点云模型提取了轨道扣件的结构特征信息,建立了轨道扣件缺陷检测组合分类器模型,实现了轨道扣件的弹条缺失、扣件歪斜、螺母缺失等缺陷检测。研究了基于表面法向量的螺母上平面解析方法,通过螺母松动测量实验实现了轨道扣件的松动检测。搭建了扣件故障诊断实验平台并开展了相关实验研究,实验结果表明,系统扣件故障检出率达到 96%,扣件松紧度测量的总体误差低于 0.2 mm,扣件故障诊断系统的检测效果和鲁棒性较好,对列车安全运行具有重要的现实意义。

**关键词** 测量; 三维图像处理; 轨道扣件; 线结构光; 中心线提取; 故障诊断  
中图分类号 TP274 文献标志码 A

DOI: 10.3788/CJL231053

## 1 引言

轨道扣件是轨道结构的重要组成部分,其服役状态直接决定了列车的运维状态,因此,扣件的故障诊断是铁路设施维护的重要环节<sup>[1]</sup>。轨道扣件故障的表现形式主要为扣件缺陷和松动,缺陷表现为零件缺失、安装错误等,松动表现为扣件离缝。现阶段,轨道扣件故障诊断主要采用机器视觉结合智能算法对扣件进行图像检测,图像检测分析主要分为二维图像识别和三维图像重构分析。二维图像识别由于受环境背景要求高、缺陷识别能力弱等限制,存在微小缺陷检测精度低、扣件离缝检测难、误报率高等问题,因此目前大多检测方法以三维图像重构分析为主。近年来,针对轨道扣件故障诊断,国内外学者利用机器视觉基于三维图像重构分析进行了大量研究。Lorente 等<sup>[2]</sup>提出了基于三维迭代最近点匹配法的扣件故障诊断方法,根据先验知识提取扣件点云与预设扣件点云进行匹配,从而实现扣件故障诊断。陈文婷等<sup>[3]</sup>以道钉与螺母的整体深度参数作为扣件松紧度的检测阈值,实现了对扣件松动的检测,但检测精度相对较低。Mao 等<sup>[4]</sup>利用线结构光传感器构建扣件的表面三维点云,通过决策树分类器对故障缺陷进行分类,并评估了扣件的松紧度,该方法检测精度较高,但计算复杂且易受噪声影响。Han 等<sup>[5]</sup>利用基于二维灰度和三维深度信息的扣件图像,对螺母和螺栓相对于轨面的位置进行分析以计算扣件松紧度,检测精度达 0.5 mm,但该方法较难

适应轨面高度变化。李明森等<sup>[6]</sup>使用改进灰度权重模型法精确提取线结构光中心线,通过 K 均值聚类法对三维重构的扣件进行缺损检测,此方法对扣件缺失的检测效果较好,但不适用于阴暗潮湿环境。

精准重构扣件三维点云是实现扣件故障诊断的关键,扣件表面结构复杂、线结构光分布零散导致线结构光中心线的精准提取比较困难。国内外学者针对复杂环境下的中心线提取进行了相关研究<sup>[7-10]</sup>,目前中心线提取常用方法有极值法<sup>[11]</sup>、灰度重心法<sup>[12]</sup>、Steger 算法<sup>[13]</sup>等。以上方法在线结构光分布复杂时不能准确提取中心线,较难适应不同宽度和噪声幅度的光条纹,且难以兼顾普适性、稳定性,重构后的扣件点云模型存在噪点且精度较差,导致扣件故障诊断时检测精度较低、鲁棒性不高。

因此,本文研究了一种基于改进灰度重心法的光条中心线提取方法,精准重构了轨道扣件点云模型。基于点云模型提取了轨道扣件的结构特征信息,建立了轨道扣件缺陷检测组合分类器模型,实现了轨道扣件的弹条缺失、扣件歪斜、螺母缺失等缺陷的检测。研究了基于表面法向量的螺母上平面解析方法,通过螺母松动测量实验实现了轨道扣件的松动检测。

## 2 基于改进灰度重心法的轨道扣件三维重构

## 2.1 线结构光测量原理分析

线结构光传感器主要由线结构光发射器与工业

收稿日期: 2023-07-24; 修回日期: 2023-09-03; 录用日期: 2023-10-11; 网络首发日期: 2023-11-13

基金项目: 国家自然科学基金青年科学基金(52105542)、“成渝地区双城经济圈建设”科技创新项目(KJCX2020032)、重庆市教委科学技术研究项目(KJZD-K202200705)

通信作者: \*ssz091011@163.com

相机构成,采用线面模型进行测量。如图 1(a)所示,在线结构光线面测量模型中,空间中光条上的任何一点  $P$  在相机成像平面上形成像点  $p$ ,线  $O_c p$  为经过像点  $p$  的唯一过光心的射线,面为结构光投射的光平面,求解出射线方程和光平面方程的参数,二者交

点  $P$  的空间三维坐标就能被唯一确定。其中,  $O_w X_w Y_w Z_w$  为世界坐标系,  $O_c x_c y_c z_c$  为相机坐标系,  $Ouv$  为图像坐标系,  $OXYZ$  为轨检车坐标系 ( $X$  轴垂直于钢轨方向,  $Y$  轴方向为扫描方向,  $Z$  轴方向为高度方向)。

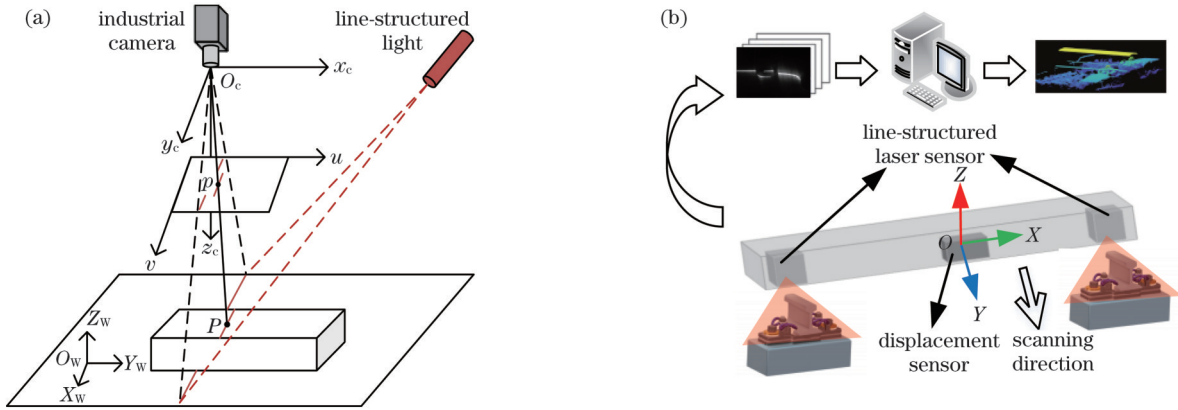


图 1 轨道扣件检测系统。(a)线面测量模型;(b)系统结构图

Fig. 1 Rail fastening detection system. (a) Line-surface measurement model; (b) system structure diagram

基于线结构光的扣件故障诊断系统由计算机、线结构光传感器和移动平台组成,如图 1(b)所示。线结构光传感器投射出线结构光,光线在扣件表面上形成调制光条纹。工业相机采集带有光条纹的图像并传输至计算机,通过计算机对图像进行处理提取出光条纹中心线;根据测量系统的数学模型,计算光条纹上点的真实坐标,通过拼接连续位置的光条纹点云还原扣件的三维轮廓;最后扣件故障诊断系统根据扣件三维点云模型进行故障诊断。

### 2.2 基于改进灰度重心法的中心线提取

线结构光光条纹经轨道扣件调制后分布在不同平面交界处,受环境光照强度、扣件表面污渍等影响,图像整体灰度、光条亮度、光条宽度不一致且存在噪点,导致光条中心线提取不精准。因此,本文研究了基于改进灰度重心法的中心线提取方法,以精准提取光条中心线。

为了降低环境光照对图像质量的影响,在镜头

上加装红光滤波片和减光片进行光学滤波,采用高斯滤波滤除光条纹灰度图中的噪声,使光条纹灰度分布更加均匀。设光条纹图像的像素有  $i$  行  $j$  列,遍历第  $j$  列像素灰度值,根据该列像素的最大灰度值 ( $G_{max}$ ) 与平均灰度值 ( $G_{avg}$ ) 计算自适应分割阈值 ( $T_{Th}$ ),计算表达式为

$$T_{Th} = KG_{max} + (1 - K)G_{avg}, \quad (1)$$

式中:  $K$  为阈值校正系数。若计算的阈值  $T_{Th}$  与  $G_{avg}$  相近,则进行下一列的像素灰度值遍历;反之,保存灰度值大于分割阈值的像素点行坐标与灰度值,完成光条的粗提取。

在相邻两个像素点与相应的灰度值之间分别进行线性插值细化,如图 2(a)所示,若该列有  $n$  个满足条件的像素点,设其中第  $k$  个像素点行坐标为  $y_k$ ,灰度值为  $G_k$ ,第  $k+1$  个像素点的行坐标为  $y_{k+1}$ ,灰度值为  $G_{k+1}$ ,则插入  $r$  个点中第  $x$  个点的行坐标  $y_x$  与灰度值  $G_x$  分别为

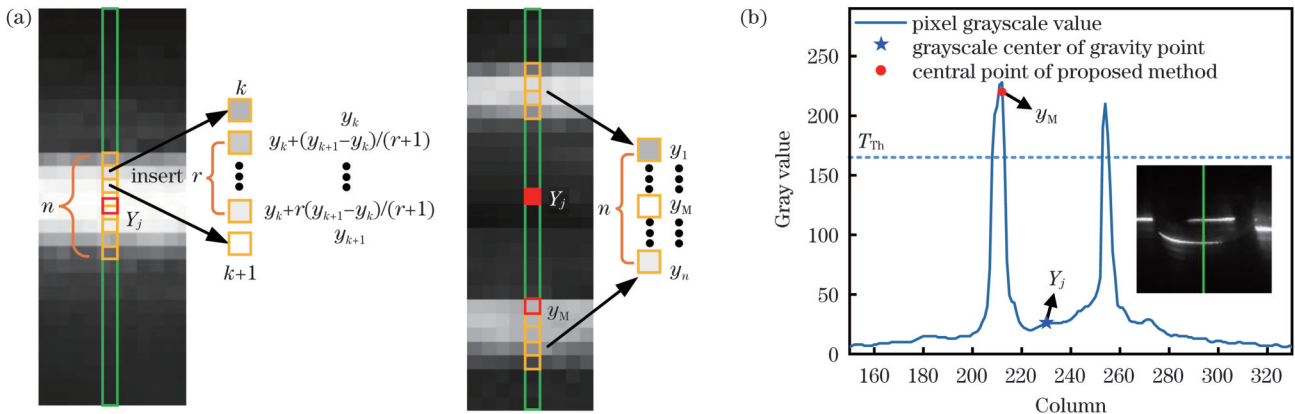


图 2 算法原理图。(a)中心点提取;(b)交界处光条灰度分布

Fig. 2 Schematics of algorithm. (a) Center point extraction; (b) light bar grayscale distribution at junction

$$\begin{cases} y_x = y_k + x(y_{k+1} - y_k)/(r+1) \\ G_x = G_k + x(G_{k+1} - G_k)/(r+1) \end{cases} \quad (2)$$

式中:  $x \in \{1, 2, \dots, r\}$ 。因此,第  $j$  列在进行线性插值后共有  $n + (n-1)r$  个满足阈值条件的点,则中心点行坐标计算表达式为

$$Y_j = \left( \sum_{m=1}^{n+(n-1)r} y_m \cdot G_m \right) / \left( \sum_{m=1}^{n+(n-1)r} G_m \right), \quad (3)$$

式中:  $Y_j$  为该列光条的中心点行坐标;  $y_m$  为像素点行坐标;  $G_m$  为灰度值;  $m$  为像素点编号,  $m=1, 2, \dots, n+(n-1)r$ 。若该列光条位于两平面交界处,则取这  $n$  个点的中位数行坐标  $y_M$  作为中心点的行坐标  $Y_j$  进行校正。

分别用极值法、灰度重心法、Steger法和本文方法进行光条中心提取,结果如图3所示。

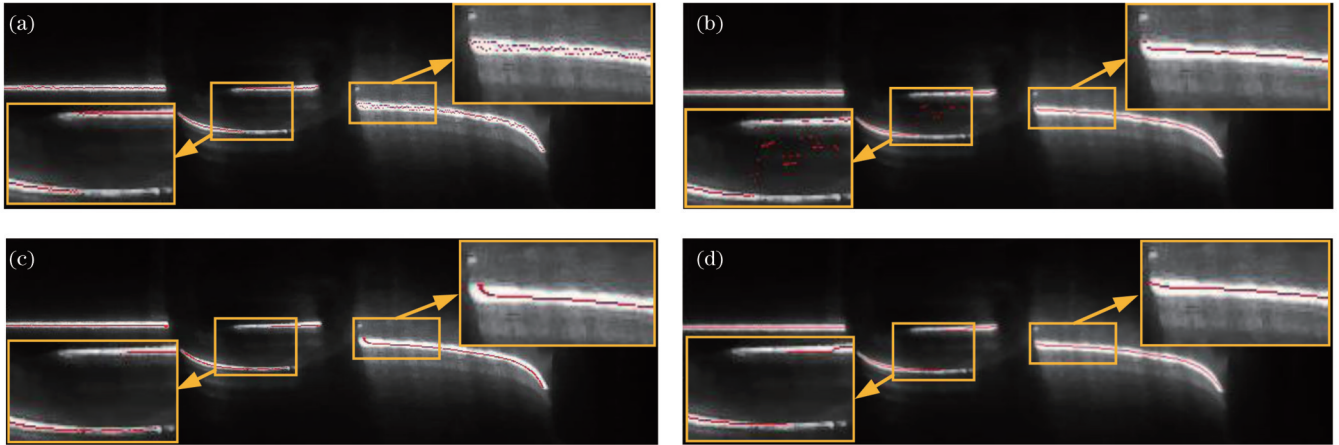


图3 不同算法中心线提取结果。(a)极值法;(b)灰度重心法;(c)Steger法;(d)本文方法

Fig. 3 Results of centerline extraction using different algorithms. (a) Extreme value method; (b) grayscale center of gravity method; (c) Steger method; (d) proposed method

### 2.3 不同影响条件下中心线提取对比

为验证改进灰度重心法的中心线提取方法的可行性与鲁棒性,分别在无光照、LED光照、正常环境光照和扣件表面存在污渍的情况下,采用改进算法对扣件

调制后的光条进行中心线提取,对比结果如图4所示,可以看出,改进的算法在不同影响条件下鲁棒性较好。

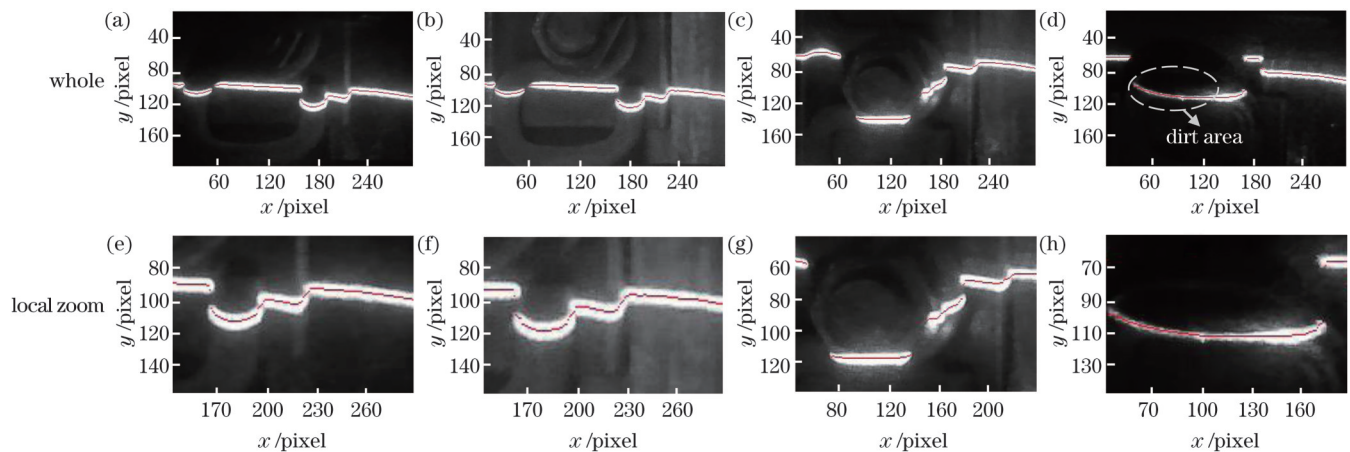


图4 不同影响条件下中心线提取的结果。(a)(e)无光照;(b)(f)LED光照;(c)(g)正常环境光照;(d)(h)存在污渍

Fig. 4 Centerline extraction results under different influence conditions. (a)(e) No lighting; (b)(f) LED lighting; (c)(g) normal ambient lighting; (d)(h) presence of stain

### 2.4 轨道扣件三维重构

线结构光测量系统经过标定后,根据测量系统的数学模型计算提取的光条中心世界坐标,结合检测系统的空间位置变化信息,拼接连续位置的中心线得到扣件点云模型<sup>[14]</sup>。采用常见算法与本文算法对扣件进

行三维重构对比,结果如图5所示,可以看出,常见算法重构的扣件点云模型存在较多噪声点、精度低,不利于扣件故障诊断分析,而基于改进灰度重心法重构的扣件点云模型无噪点、精度高,为扣件的故障诊断提供了精确的点云模型。

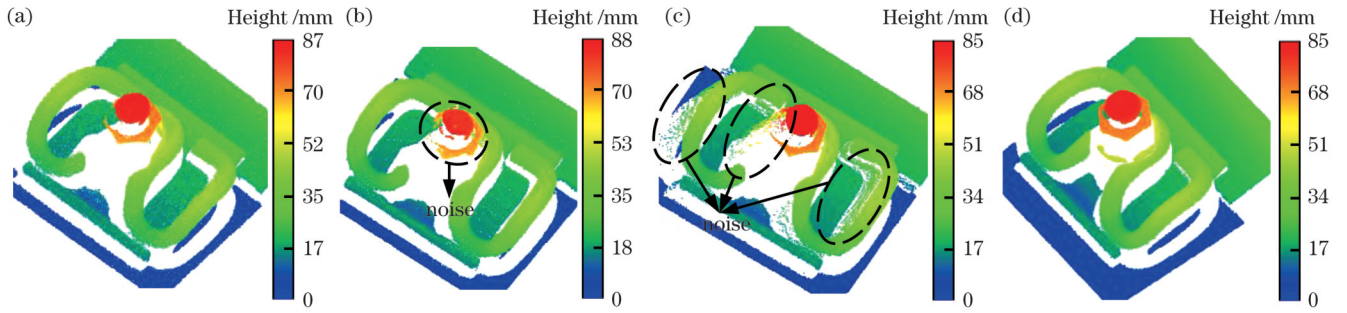


图 5 扣件三维重构结果。(a)极值法;(b)Steger法;(c)灰度重心法;(d)本文方法

Fig. 5 3D reconstruction results of fastener. (a) Extreme value method; (b) Steger method; (c) grayscale center of gravity method; (d) proposed method

### 3 轨道扣件故障诊断

#### 3.1 扣件检测坐标系建立

本文以弹条 I 型分开式扣件为研究对象,该扣件结构如图 6(a)所示,主要由螺母、螺栓、弹条、轨距挡板、平垫圈、挡板座等部件组成。弹条通过螺母将轨距挡板固定,防止钢轨产生横移,因此弹条和螺母是扣件故障诊断中的重点检测对象。扣件三维点云

模型的最高位置为中心螺栓上表面,其离钢轨底面的高度相对固定,因此可根据点云最高位置进行扣件粗定位。通过随机采样一致性(RANSAC)算法对螺栓表面点云进行圆形拟合,计算圆心坐标,并将圆心作为扣件检测坐标系原点  $o$ ,如图 6(c)所示,设定扣件检测坐标系  $x$  轴平行于钢轨,方向与检测方向一致; $y$  轴垂直于钢轨,方向指向钢轨; $z$  轴与高度方向一致。

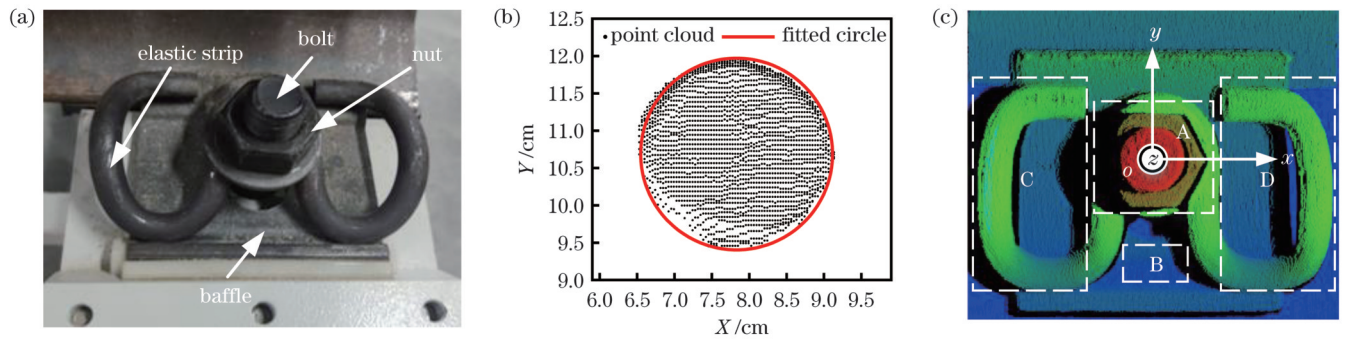


图 6 扣件坐标系的建立。(a)扣件实物图;(b)螺栓上表面圆形拟合;(c)扣件检测坐标系

Fig. 6 Establishment of fastener coordinate system. (a) Physical drawing of fastener; (b) circular fitting of upper surface of bolt; (c) fastener detection coordinate system

#### 3.2 轨道扣件缺陷检测

结合扣件结构特征与高度信息,根据扣件结构和零部件间的拓扑关系设计组合分类器,对扣件缺陷进行精细化检测分类。如图 6(c)所示,在检测区域 A 中通过平面拟合检测螺母上表面,进而判断螺母是否存在;在检测区域 B 中根据点云数量及位置判断扣件安装方向;在检测区域 C、D 中,根据点云数量检测弹条的缺失;通过提取 C、D 区域的弹条点云并计算其与扣件坐标系  $x$  轴的偏转角度  $\theta$ ,实现扣件歪斜检测。构建的组合分类器如图 7 所示。

由于扣件为不规则几何体,难以计算扣件的偏转角度,而根据弹条两侧点云高度分布图可知,部分点云在扣件偏转过程中始终处于检测区域 C、D 中的最高位置,如图 8(a)所示。因此,提取弹条两侧 2/3 以上高度位置的点云作为检测区域的特征点云,如图 8(b)所示,将所要拟合的点云映射在扣件检测坐标系中的

$xoy$  平面坐标系下,采用最小二乘法进行直线拟合,拟合的直线与  $x$  轴之间的夹角  $\theta$  计算式为

$$\theta = \arctan\left(\frac{k_0 - k'}{1 + k'k_0}\right), \quad (4)$$

式中: $k_0$  为  $xoy$  平面中  $x$  轴的斜率,大小为 0; $k'$  为拟合直线在  $xoy$  平面坐标系中的斜率。若计算的扣件歪斜角度大于  $5^\circ$ ,则认为扣件存在歪斜。

#### 3.3 轨道扣件松紧度检测

松动的扣件弹条与压板之间会产生离缝间隙( $h$ ),且扣件螺母向上发生纵向位移,如图 9(a)所示。正常情况下扣件离缝距离应小于 2 mm,过大的扣件离缝距离难以产生足够的扣压力<sup>[15]</sup>。由于弹条表面为复杂曲面,难以直接测量扣件离缝距离,而完全拧紧的扣件螺母上表面与挡板的距离( $H_0$ )固定,因此可通过计算螺母上表面与挡板的距离实现扣件松动检测。

解析螺母上表面所在的平面是螺母松动检测的关

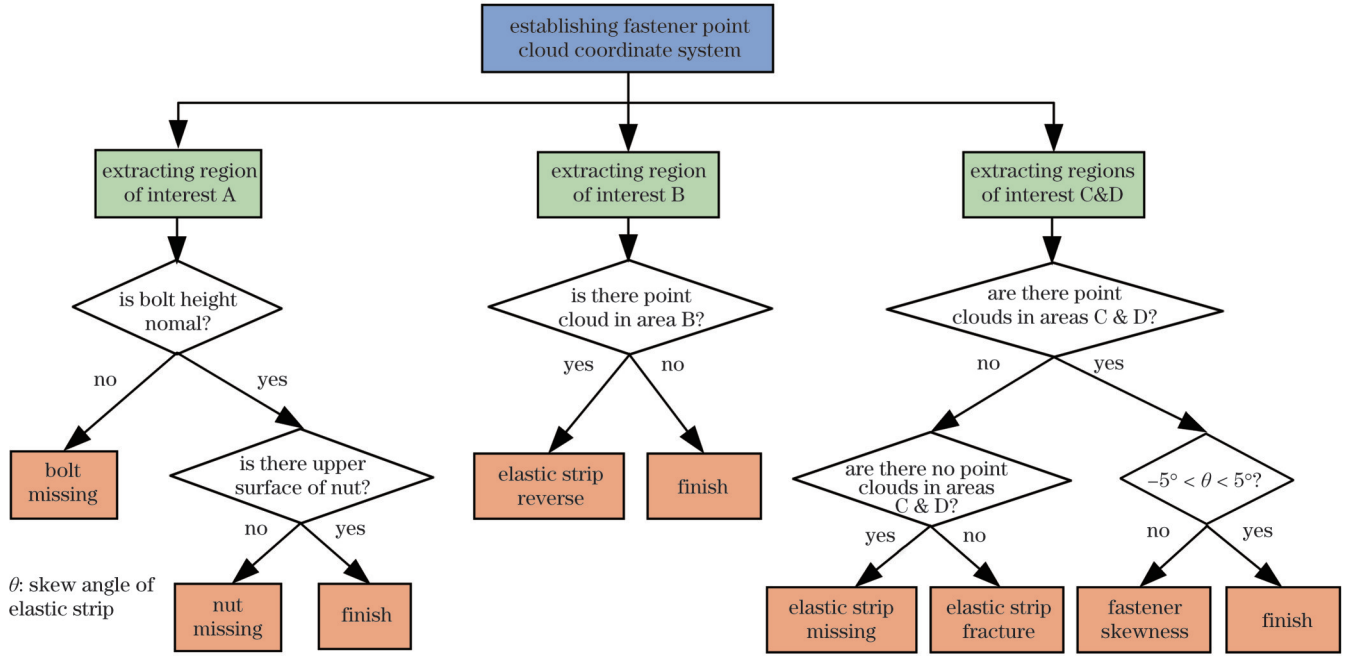


图 7 扣件缺陷检测组合分类器模型

Fig. 7 Combined classifier model of fastener defect detection

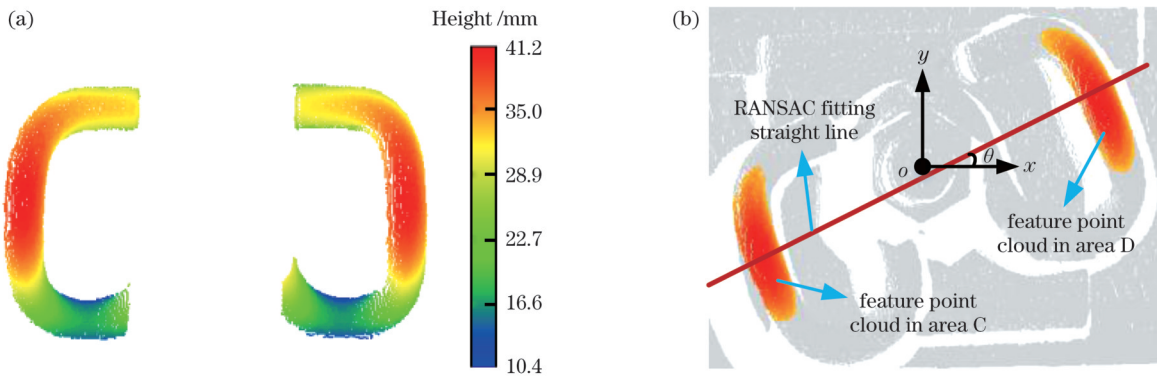


图 8 扣件歪斜检测。(a)C、D 两区域的点云高度分布；(b)歪斜检测原理图

Fig. 8 Inspection for skewness of fastener. (a) Height distribution of point clouds in areas C and D; (b) detection diagram of skewness

键,因此,本文研究了基于表面法向量的点云分割算法,根据检测区域 A 中点云的法向量与欧氏距离分割提取螺母和螺栓上表面,根据高度位置信息解析螺母上表面。

首先,解析螺母上表面。利用扣件坐标系设置螺母松动检测区域 A,分割出包含螺栓和螺母的点云数

据。估算该部分点云的法向量与曲率作为局部特征,如图 9(b)所示,滤除法向量非竖直向上和曲率变化较大的点。基于 RANSAC 方法拟合出螺母和螺栓上表面,根据平面高度位置解析螺母上表面所在平面(S),记为  $A'x' + B'y' + C'z' + D' = 0$ ,其中,  $A', B', C', D'$  为拟合的平面方程系数,  $x', y', z'$  为拟合点的三维坐标值。

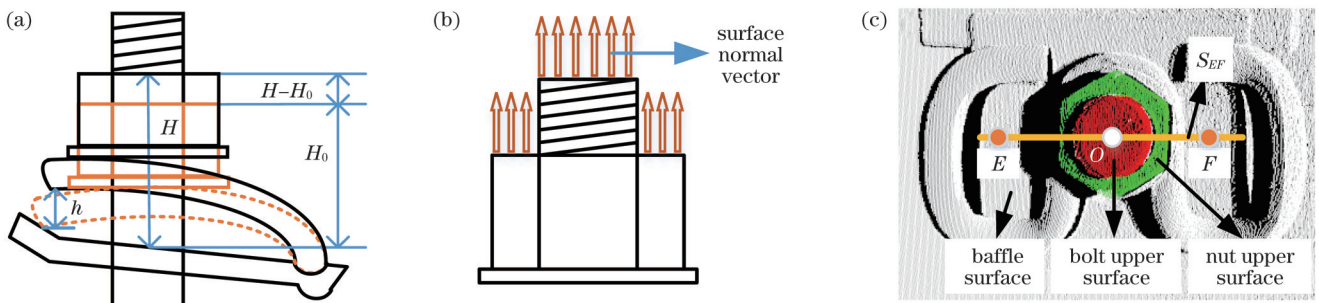


图 9 扣件松动检测。(a)检测原理；(b)表面法向量估计；(c)螺母松动检测示意图

Fig. 9 Looseness detection of fastener. (a) Detection principle; (b) surface normal vector estimation; (c) detection diagram of nut looseness

其次,计算螺母上平面高度。如图 9(c)所示,在经过扣件坐标系  $x$  轴且垂直于螺母上表面的平面 ( $S_{EF}$ )与挡板表面相交的位置上设置检测基准点  $E$ 、 $F$ ,通过提取检测点  $E$ 、 $F$ 的空间位置信息,分别计算到平面  $S$  的距离  $H_E$ 、 $H_F$ ,取二者的平均值作为螺母上表面到挡板的距离 ( $H$ ),  $H_x$  取  $H_E$ 、 $H_F$ ,  $(x_0, y_0, z_0)$  为检测基准点的三维坐标,则距离计算式为

$$\begin{cases} H_x = \frac{A'x_0 + B'y_0 + C'z_0 + D'}{\sqrt{A'^2 + B'^2 + C'^2}} \\ H = \frac{H_E + H_F}{2} \end{cases} \quad (5)$$

最后,计算弹条离缝距离。弹条离缝距离计算表达式为

$$h = (H - H_0) \cdot K_0, \quad (6)$$

式中:  $K_0$  为转换系数。将螺母松动值转换为弹条离缝距离,经过多次实验测量计算  $H_0$  取 49.00 mm,  $K_0$  取 1.162。若  $h < 2$  mm,则扣件松紧度适中;若  $h > 2$  mm,则记录该扣件位置信息。

### 4 实验结果分析

为检测线结构光测量系统的精度,本文设计搭建线结构光测量设备,相机景深范围为 300~450 mm,采集的图像大小为 1920 pixel × 1080 pixel,对高度分别为  $(20 \pm 0.02)$  mm、 $(60 \pm 0.02)$  mm、 $(100 \pm 0.02)$  mm 的标准块进行三次高度测量并取平均值,结果如表 1 所示。

精度检测结果表明,系统测量总体误差低于 0.2 mm,满足检测需求。图 10 为数据采集设备,使用巡检车扣件检测系统对 100 个正常扣件和 100 个故障扣件进行

表 1 精度检测实验结果

Table 1 Precision detection experimental results

unit: mm			
Block height	Average height	Standard deviation	Absolute error
20	19.85	0.08	0.15
60	59.88	0.06	0.12
100	99.90	0.05	0.10

诊断,其中故障扣件包含弹条缺损、弹条装反、扣件歪斜、螺母丢失、松紧程度不同的扣件各 20 个,实验结果如图 11 和图 12 所示。

由图 12(a)可知,在扣件缺陷检测实验中,正常扣件中有 2 个扣件误检为缺陷扣件,弹条装反和歪斜的扣件分别有 1 个未检测出,螺母丢失的扣件有 2 个未检测出,系统总共成功检测出缺陷扣件 76 个,误检测扣件 6 个。由图 12(b)可知,在 20 个扣件松紧度检测实验中,诊断系统检测出松动扣件 17 个,与人工判定结果相符,最大检测误差为 0.18 mm。整体上诊断系统故障检出率为 96%,误诊断率为 3%。

为检验系统工作的鲁棒性,选取部分含有灰尘、油污的 200 个轨道扣件,其中包含 80 个缺陷扣件、20 个松动扣件,分别在不同光照强度条件下对轨道扣件进行扫描重构及故障诊断,扣件故障诊断结果如表 2 所示。

由测试结果可知,系统在黑暗环境下时扣件故障检出率最高,而在有外部光源照射干扰时系统采集的光条图像含有较多噪声数据从而产生误检,整体上系统受不同环境光照强度和扣件表面污渍的影响较小,系统的鲁棒性较强。

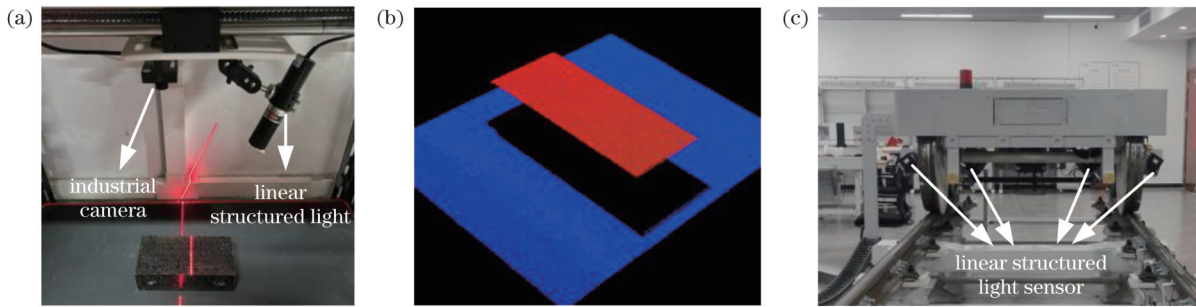


图 10 数据采集设备。(a)室内采集设备;(b)标准块点云;(c)巡检车采集设备

Fig. 10 Data collection devices. (a) Indoor collection equipment; (b) standard block point cloud; (c) inspection vehicle collection equipment

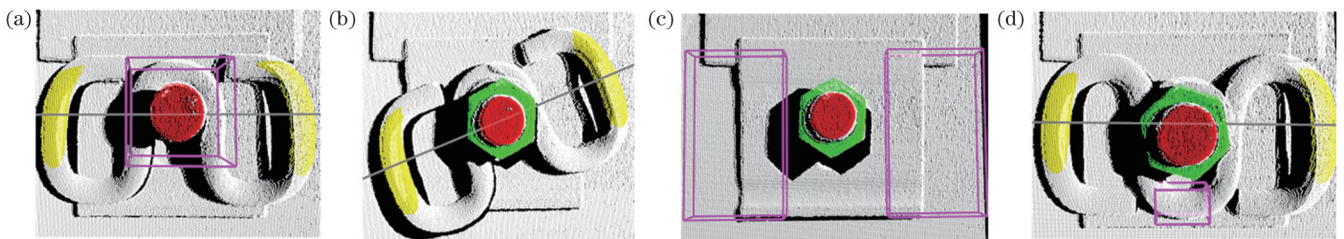


图 11 故障诊断。(a)螺母丢失;(b)扣件歪斜;(c)弹条丢失;(d)弹条装反

Fig. 11 Fault diagnosis. (a) Nut missing; (b) fastener skewness; (c) elastic strip missing; (d) elastic strip reverse

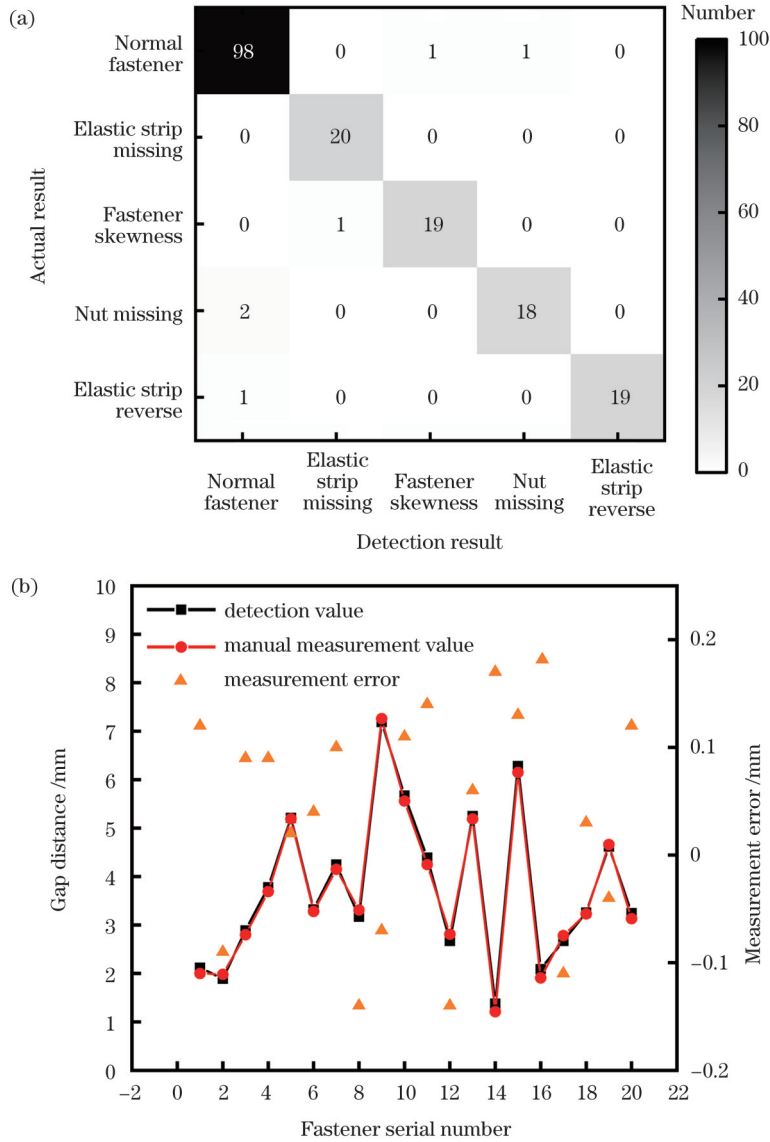


图 12 实验结果。(a)扣件缺陷检测;(b)扣件松紧度检测

Fig. 12 Experimental results. (a) Defect detection of fastener; (b) tightness detection of fastener

表 2 系统鲁棒性测试结果

Table 2 System robustness test results

Condition	Number of successful diagnoses	Number of misdiagnosis	Fault detection rate /%	Diagnostic error rate /%
Darkness	98	4	98	2.0
Environment lighting	96	6	96	3.0
LED lighting	95	7	95	3.5

## 5 结 论

针对三维图像的扣件故障诊断参数不全面、检测精度较低等问题,设计搭建了基于线结构光的轨道扣件故障诊断系统,对弹条 I 型分开式扣件进行扫描重构与故障诊断。首先针对经扣件调制后的光条中心线提取困难的问题,研究了一种基于改进灰度重心法的中心线提取方法,精准地重构了扣件点云模型;其次建

立了一种扣件缺陷检测组合分类器模型,实现了扣件缺陷检测;最后通过对扣件螺母松动进行测量,实现了扣件松动检测,解决了扣件离缝难以直接测量的问题。实验结果表明,在正常光照环境下诊断系统故障检出率为 96%,扣件松动检测误差低于 0.2 mm。扣件故障诊断模型具有较好的检测效果与鲁棒性,对及时发现故障扣件并进行维修、保障列车的安全运行具有重要现实意义。

## 参 考 文 献

- [1] 刘甲甲, 熊鹰, 李柏林, 等. 基于计算机视觉的轨道扣件缺陷自动检测算法研究[J]. 铁道学报, 2016, 38(8): 73-80.  
Liu J J, Xiong Y, Li B L, et al. Research on automatic inspection algorithm for railway fastener defects based on computer vision[J]. Journal of the China Railway Society, 2016, 38(8): 73-80.
- [2] Lorente A G, Llorca D F, Velasco M G, et al. Detection of range-based rail gage and missing rail fasteners: use of high-resolution two- and three-dimensional images[J]. Transportation Research Record: Journal of the Transportation Research Board, 2014, 2448(1): 125-132.
- [3] 陈文婷, 罗文婷, 李林, 等. 基于 2D 与 3D 激光图像的轨道扣件状态智能检测[J]. 仪表技术与传感器, 2022(11): 88-95.  
Chen W T, Luo W T, Li L, et al. Intelligent detection of rail fastener state based on 2D and 3D laser images[J]. Instrument Technique and Sensor, 2022(11): 88-95.
- [4] Mao Q Z, Cui H, Hu Q W, et al. A rigorous fastener inspection approach for high-speed railway from structured light sensors[J]. ISPRS Journal of Photogrammetry and Remote Sensing, 2018, 143: 249-267.
- [5] Han Q, Wang S C, Fang Y, et al. A rail fastener tightness detection approach using multi-source visual sensor[J]. Sensors, 2020, 20(5): 1367.
- [6] 李明森, 李林, 张超, 等. 基于三维激光成像技术的扣件缺损自动检测[J]. 激光与红外, 2022, 52(5): 670-677.  
Li M S, Li L, Zhang C, et al. Automatic detection of fastener defects based on 3D laser imaging technology[J]. Laser & Infrared, 2022, 52(5): 670-677.
- [7] Wan Z R, Lai L J, Mao J, et al. Extraction and segmentation method of laser stripe in linear structured light scanner[J]. Optical Engineering, 2021, 60(4): 046104.
- [8] 张倩, 张坤, 朱美强, 等. 运动模糊情况下的结构光光条中心快速提取[J]. 激光与光电子学进展, 2023, 60(1): 0112002.  
Zhang Q, Zhang K, Zhu M Q, et al. Fast extraction of structure light strip center under motion blur[J]. Laser & Optoelectronics Progress, 2023, 60(1): 0112002.
- [9] 李伟明, 彭国, 高兴宇, 等. 线激光光条中心快速提取算法[J]. 中国激光, 2020, 47(3): 0304002.  
Li W M, Peng G, Gao X Y, et al. Fast extraction algorithm for line laser strip centers[J]. Chinese Journal of Lasers, 2020, 47(3): 0304002.
- [10] 王胜春, 韩强, 王昊, 等. 行车环境下钢轨轮廓激光条纹中心的提取方法[J]. 光学学报, 2019, 39(2): 0212004.  
Wang S C, Han Q, Wang H, et al. Laser stripe center extraction method of rail profile in train-running environment[J]. Acta Optica Sinica, 2019, 39(2): 0212004.
- [11] 周渊, 孟祥群, 江登表, 等. 复杂干扰情况下的结构光条纹中心提取方法[J]. 中国激光, 2020, 47(12): 1204004.  
Zhou Y, Meng X Q, Jiang D B, et al. Centerline extraction of structured light stripe under complex interference[J]. Chinese Journal of Lasers, 2020, 47(12): 1204004.
- [12] 胡杨, 方素平. 线结构光条纹中心提取方法[J]. 激光与光电子学进展, 2021, 58(1): 0112005.  
Hu Y, Fang S P. Extraction method of light stripe center of linear structure[J]. Laser & Optoelectronics Progress, 2021, 58(1): 0112005.
- [13] 蔡怀宇, 冯召东, 黄战华. 基于主成分分析的结构光条纹中心提取方法[J]. 中国激光, 2015, 42(3): 0308006.  
Cai H Y, Feng Z D, Huang Z H. Centerline extraction of structured light stripe based on principal component analysis[J]. Chinese Journal of Lasers, 2015, 42(3): 0308006.
- [14] 王海. 基于线结构光三维测量方法的研究[D]. 上海: 东华大学, 2022.  
Wang H. Research on three-dimensional measurement method based on line structured light[D]. Shanghai: Donghua University, 2022.
- [15] 崔昊. 基于结构光点云的轨道扣件服役状态检测关键技术研究[D]. 武汉: 武汉大学, 2019.  
Cui H. Research on key technologies of track fastener service condition detection based on structured light point cloud[D]. Wuhan: Wuhan University, 2019.

## Reconstruction of Rail Fasteners and Fault Diagnosis Based on Improved Grayscale Gravity Center Method

Xiao Zhen, Sun Shizheng\*, Zheng Tiancheng, Pang Ke, Wei Zijie

College of Mechanical and Electrical Engineering, Chongqing Jiaotong University, Chongqing 400074, China

### Abstract

**Objective** The status detection of track fasteners is an important task in railway facility inspection and maintenance. Fastener failures mainly manifest in defects such as missing, damage, incorrect installation of fastener components, and looseness of fasteners. Faulty fasteners can cause changes in track parameters, posing significant safety hazards. Therefore, strengthening the status detection of track fasteners has important practical significance for ensuring the safe operation of trains. At present, many researchers have conducted fault diagnosis research on fastener status based on 2D and 3D images. The fault detection of fasteners based on 2D images is greatly affected by factors such as lighting conditions, environmental background, and the ability to identify small defects in fasteners; moreover, depth information is not available, making it difficult to detect the tightness of fasteners. The detection accuracy based on 3D image data is low and there is a single detection parameter. Research in this area is relatively limited and immature. Based on line-structured light for detection, the distribution of the light strip modulated by the surface of the track fastener is scattered and affected by different environmental light intensities and surface stains of the fastener. Existing methods for extracting the centerline of line-structured light cannot simultaneously consider universality, accuracy, and robustness, making it difficult to accurately extract the centerline of the light strip. The reconstructed point cloud model of the fastener has many noisy points and poor accuracy, which makes it difficult to diagnose fastener faults. Therefore, this article reports on a light strip centerline extraction method and fastener fault diagnosis method suitable for precise reconstruction of track fasteners. The objective is to realize high-



precision and high-robustness fault diagnosis of track fasteners, timely eliminating safety hazards and ensuring reliable service of fasteners and safe operation of trains.

**Methods** In response to the difficulty in accurately extracting the centerline of the line-structured light strip modulated by track fasteners, this study proposes a centerline extraction method based on the improved grayscale center of the gravity method. This method mainly consists of four steps. First, a filter is used to maintain the overall grayscale stability of the image, making the light stripe image brighter. Gaussian filtering is used to filter out noise in the image, while making the distribution of light stripes uniform and closer to a Gaussian distribution. Second, an adaptive segmentation threshold for light stripe segmentation is calculated to reduce the impacts of different lighting intensities and surface stains on the centerline extraction, effectively completing the coarse extraction of light stripes. Third, linear interpolation is performed between the adjacent pixel points of the light strip in coarse extraction to refine the grayscale distribution of the light strip. The center point of the light strip is calculated using the grayscale center of the gravity method to accurately extract the centerline. Finally, the extracted center point is checked; if the point is not located on the light strip, the median pixel that meets the conditions is used as the center point of the light strip for correction. The feasibility and robustness of the proposed method are verified by comparing the experimental results of centerline extraction under different influencing conditions. This study is based on the reconstructed fastener point cloud model. By constructing a detection combination classifier of fastener defects, different defective fasteners can be diagnosed and classified. By measuring the looseness value of the nut, the distance between the fastener and the seam is indirectly measured to achieve fastener looseness detection.

**Results and Discussions** An accuracy detection experiment is conducted on the fault diagnosis system of the elastic strip I-type split fastener by building an indoor structured light sensor. The experimental results show that the overall measurement error of the system is less than 0.2 mm (Table 1). Subsequently, 100 normal fasteners and 100 faulty fasteners are diagnosed under normal lighting conditions using a structured light sensor device on the inspection vehicle line. The experimental results show that the system has a fastener fault detection rate of 96%, a misdiagnosis rate of 3% [Fig. 12(a)], and a maximum error of 0.18 mm in fastener tightness detection [Fig. 12(b)]. Finally, by conducting fault diagnosis on track fasteners with surface stains under different environmental light intensity conditions, the experimental results show that the overall system is less affected by different environmental light intensities and surface stains on the fasteners (Table 2), and the system has strong robustness and fault diagnosis ability, meeting the detection requirements of track fasteners.

**Conclusions** Currently, the fault diagnosis parameters for fasteners based on 3D images are not comprehensive and the detection accuracy is low. There is scarce and immature research in this area. Therefore, this study independently designs and builds a track fastener fault diagnosis system based on line-structured light to scan, reconstruct, and diagnose the elastic strip I-type split fastener. First, in response to the difficulty in extracting the centerline of the light strip modulated by fasteners, a centerline extraction method based on the improved grayscale center of the gravity method is studied, and the fastener point cloud model is accurately reconstructed. Second, a combined classifier model for fastener defect detection is established to achieve fastener defect detection. Finally, by measuring the looseness of the fastening nut, the problem of difficult direct measurement of the fastening gap is solved. The experimental results show that under normal lighting conditions, the fault detection rate of the diagnostic system is 96%, and the detection error of fastener looseness is less than 0.2 mm. The fastener fault diagnosis model has good detection performance and robustness, which is of great practical significance for timely detection and maintenance of faulty fasteners, thereby ensuring safe operation of trains.

**Key words** measurement; three-dimensional image processing; rail fastener; linear structured light; centreline extraction; fault diagnosis